Integration of tolerances in the mechanical product process: Assembly with defects modelling

M. TLIJA[a], B. LOUHICHI[a, b], A. BENAMARA[a]

a. Mechanical Engineering Laboratory, National Engineering School of Monastir, Monastir University, Av. Ibn Eljazzar, 5019 Monastir, Tunisia.
a, b. LIPPS, ÉTS, 1100, Notre-Dame Ouest, Montréal, H3C1K3, Québec, Canada.
Borhen.louhichi@etsmtl.ca, abdelmajid.benamara@enim.rnu.tn

Abstract:

The part and assembly requirements are specified by the tolerances. In the Digital Mock-Up (DMU), the product is designed on nominal configuration and the tolerances are formally allocated to the CAD model. Thus, the impacts of the tolerance stack-up on the advanced phase of the product design (Dynamic computation, F.E Analysis…) are neglected. The DMU improvement requires the tolerance integration in CAD model. A developed model allows obtaining the components with defects according to dimensional and geometrical tolerances specified in the nominal model. In CAD model, the assembly of the components with dimensional and geometrical defects requires the updating of the assembly mating constraints. This paper presents a method to redefine the mates of the realistic assemblies.

Keywords: CAD model, assembly mating constraints, dimensional tolerance, geometrical tolerance, realistic assemblies.

1 Introduction

The proper functioning of mechanical systems is controlled by Geometric Dimensioning and Tolerancing (G&DT). Current CAD systems present exhaustive capabilities for defining the numerical model of the product. However, in DMU, the tolerance integration in CAD models and the determining of the tolerance impacts on advanced phases of Product Lifecycle Management (PLM) continuous to be limited.
In literature, several methodologies of tolerance analysis and syntheses for a good choice of specifications were developed. The MECAmaster software is integrated in CATIA V5 to simulate assembly in an earlier phase of product design. This CAT (Computer aided tolerancing) software allows the three-dimensional tolerance analysis [1]. The CLIC (Tolerancing in Localization with Influence of the Contacts) method leads to choosing the optimal dimensional and geometric specifications for a mechanism [2]. CLIC is CAT software based on three-dimensional computation. In addition, Germain et al. [3] and Pillet et al. [4] were developed a static and three-dimensional tolerancing models to optimize tolerance values of functional requirements.
Socoliuc et al. established an approach to realize a realistic simulation of assemblies [5]. This approach is based on TTRS (Topologically and technologically related surfaces) model [6]. A complex mechanical system is represented by a simple parametric model. Then, the point deviations, which are located on the toleranced face, are modelled by the polyhedral tool [7]. Therefore, the tolerance effects on assembly functional requirements are obtained. Nevertheless, the polyhedral is a difficult tool to be used on industry. This model does not predict the impacts of dimensional and geometrical deviations which are permitted by tolerances, on the assembly deformations. Pierre et al. developed a method to take into account both the thermo-mechanical effects and the geometrical defects of the assembly by using the three-dimensional chain tools [8]. The model is based on the substitute surfaces approach. The model presents a solution, in torsorial form, for the problems of coupling between the thermal requests and the geometrical defects. This tool was improved by proposing a vectorial method for tolerance analysis. The model improvement was also performed by using common surfaces in contact between the assembled parts [9]. The solutions are presented in mathematical form (equations) and not modelled as a geometric solution.
In this paper, we propose a CAD modelling of the realistic assemblies. The components with dimensional and geometrical defects are first obtained according the specified tolerances by using models which were developed in our previous works [10]-[12]. The combinations of these component configurations lead to

obtain the realistic assemblies (Fig. 1 (a)). The obtained models can be easily used on advanced phase of the product design such as the motion and deformation simulations comparing to the existing methods [2]-[5]. In this document, the two algorithms to take account dimensional and geometrical tolerances are described shortly. Then, a method to update mating constraints of realistic assemblies is shown.

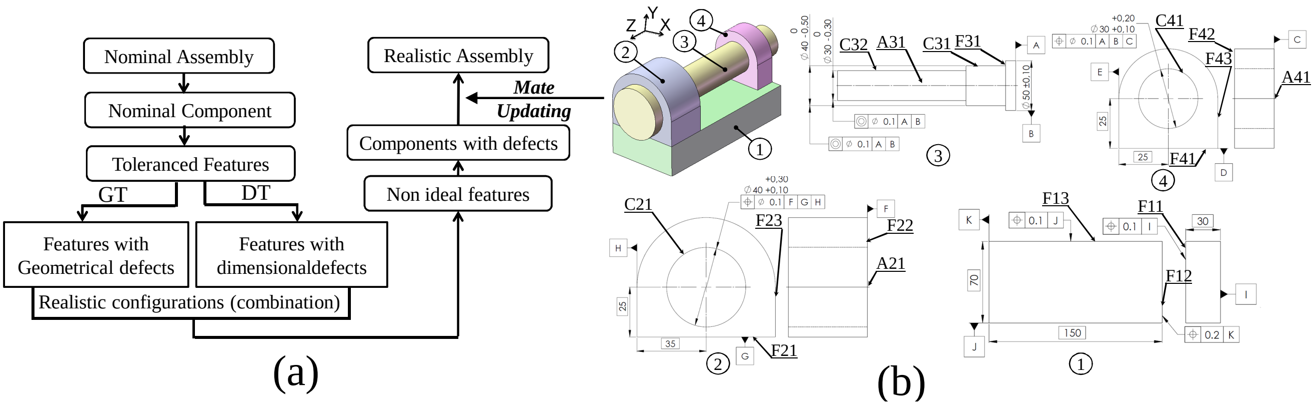

FIG. 1 – (a) Algorithm to obtain the realistic assemblies, (b) the studied mechanical system.

2 The components with dimensional and geometrical defects

The tolerance interpretations can be performed with two hypotheses: The first hypothesis suggests that worst cases assemblies are deduced from worst cases components [10]. The second hypothesis asserts that worst assemblies can be obtained by the random components. In addition, the approach allows simulating the random aspect of the produced products. In this paper, the second hypothesis is adopted. Two algorithms were developed to obtain automatically the realistic components. The first one leads to obtain component with dimensional defects. The second one is interested in the geometrical tolerances.

The algorithm to taking into account the dimensional tolerances in CAD model was developed to determine realistic components allowed by dimensional requirements. The tolerance interval *TI* specified on driven dimension RD_j (with nominal value VRD_j) is discretized by an increment *e*; such as $e=TI/h$. *h* is the discretization accuracy to be chosen by user. In CAD model, RD_j is driven by the *n* driving dimensions D_i ((with nominal values VD_i). Then, the relationships between driven and driving dimensions must be determined to obtain the target values (with the deviation $t_{kj}= ke$: k=0 to h) of the driven dimension. An influence coefficient λ_{ij} is defined. λ_{ij} is the ratio between the variation of the driving dimension δ_{VDi} and the variation of the driven dimension δ_{VRj} (Eq. 1). λ_{ij} is determined by using a numerical perturbation method [11]. For each k^{th} deviation value t_{kj} of the driven dimension RDj, the deviation value T_{ki} of the driving dimension *Di* is deduced by the relation (Eq. 2). Thus, the new values of *Di* are determined according the sign of λ_{ij} (If $\lambda_{ij} > 0$, then $D_{ki}= D_i + T_{ki}$. Else If $\lambda_{ij} < 0$ then $D_{ki}= D_i - T_{ki}$). The model is rebuilt with these new values of driving dimension to obtain components with dimensional defects.

$$\lambda_{ij} = \delta_{VDi} / \delta_{VRj} \quad (1)$$

$$T_{ki} = \left|\lambda_{ij}\right| t_{kj} \ /n \quad (2)$$

The components with geometrical defects are obtained by modelling component tolerances by displacements of the corresponding faces [11]. The setting the deviation between the nominal element and the element with default is made by analogy to the parameters defined by the SDT. Then, form deviations are neglected relative to those of orientation and position.These parameters are used to discretize the tolerance zone and to define the parameters of the faces displacements (translations and rotation). The assumption of neglect of form defects versus position and orientation defects is adopted. The developed approach depends on the shape of the tolerance zone, the geometric of toleranced feature and the tolerance type. The deviation torsor, which is based on the approach of tolerancing by SDT, defines the degrees of freedom (DoF) of toleranced feature. The model was improved to takes into consideration the maximum and the least material conditions and to respect the datum priority order in the CAD model.

3 The Assemblies with defects

In the realistic assembly, mate updating is realized by defining realistic primitive joints. These realistic joints are obtained by using coincidence mates between MGREs (Minimum Geometrical Reference Elements) [6]. The method depends on the Objective Functions of the Assembly (OFA) specified by the designer. In CAD software, the OFA is deduced from the nominal model:

- The mate order, specified in the feature manager design tree of the software, defines the mounting order of the assembly and the joint order priority.
- The kinematic status of the nominal assembly defines the DoFs which are to be conserved in the realistic model. The DoFs is identified by a method based on the graphs of primitive kinematic joints: Each assembly or sub-assembly is defined with a graph. In a graph, a node represent a part, an edge represents a primitive joint.
- The contact between the features is conserved.
- The joint type between each couple of components is respected.

The hyperstatic mechanical system (Fig. 1 (b)) will be the pilot test case along this work. In the nominal configuration, the assembly has a rotational DoF about the Z-axis. The mating constraints of this assembly, which simulate the sequential mounting order, are allocated through the following order: *L1* (Co: *F21&F11*), *L2* (Co: *F22&F12*), *L3* (Co: *F23&F13*), *L4* (Co: *F41&F11*), *L5* (Co: *F42&F12*), *L6* (Dist: *F43&F13*), *L7* (Co: *A31&A21*), *L8* (Co: *A31&A41*) and *L9* (Co: *F31&F22*). A fixed joint is defined between the two part couples (*1*, *2*) and (*1*, *4*). A revolute joint specified between the parts *2* and *3*. The parts *3* and *4* are linked by a cylindrical joint. The realistic assembly is obtained by using components with defects. These components are obtained according to the dimensional and geometrical tolerances. However, in this realistic assembly configuration, the OFA specified in the nominal configuration is no longer respected. The redefinition of the assembly constrains must be performed according to the OFA.

3.1 The case of planar joint or fixed joint performed by coincidence mates between planar faces in contact

3.1.1 A coincident constraint between planar faces

In the realistic model, a coincident constraint between two planar face, defined in nominal configuration, is specified by the coincident constraint between: plane and plane (Co: *F&F*), plane and edge (Co: *F&E*) or plane and vertex (Co: *F&V*). The constraint updating depends on the initial configuration of the two faces: in contact or without contact.

a. The case of two planar faces in contact in nominal configuration

In general case, two planar faces *f1* and *f2* of the parts *A1* and *A2* respectively are in contact. The faces *f1* and *f2* are linked by a coincident constraint in the nominal configuration. The sub-algorithm VRPTFC (to Verify Relative Position of Two Faces initially in Contact) is developed to ensure that the relative position of *f1* and *f2* is adequate (Fig. 2 (a)). *N1* and *N2* are the two normal vectors of *f1* and *f2* respectively. The vertices *Pi* (*i*=1 to 4) and *Jj* (*j*=1 to 4) are the four vertices that delimit *f1* and *f2* respectively. *Q* is the plane derived from *f2*. In the realistic configuration, both faces can have three main configurations (Fig. 2 (b)). In the first case, the following condition is satisfied: $\overrightarrow{N1}.\overrightarrow{N2} \leq 0$ and $\overrightarrow{PiJj}.\overrightarrow{N1} > 0$ for *i*, *j* = 1 to 4 (an anti-alignment relation). The two faces are in the correct configuration and the both faces do not intersect. In the second case, the condition ($\overrightarrow{N1}.\overrightarrow{N2} > 0$) is satisfied (an alignment relation). The part *A1* is rotated about the $(O,\vec{T})$ axis by an angle equal to *Π*. *O* is the center of *f1* and $\vec{T}$ is the tangential axis to *f1*. After the part rotation, the configuration of *f1* and *f2* becomes similar to the configuration in the first case. In the third case, the condition ($\overrightarrow{N1}.\overrightarrow{N2} \leq 0$ and for *i, j* = 1 to 4 and there exists a pair (k, m) such that $\overrightarrow{PkJm}.\overrightarrow{N1} < 0$) is satisfied. A coincident constraint between *f1* and the vertex *Jv* is applied temporarily (Applied to move the face then deleted from the model). The vertex *Jv* is determined by the relation (Eq. 3). Then, the model becomes one of the two previous configurations (case1 or case2).

$$\begin{cases} d_{km} = \left\| \overrightarrow{PkJm}.\overrightarrow{N1} \right\|; \text{ such as } \overrightarrow{PkJm}.\overrightarrow{N1} < 0. \\ d_v = \left\| \overrightarrow{PkJv}.\overrightarrow{N1} \right\|; \textit{ such as } d_v = \max(d_{km}); \text{ k, m =1 to 4.} \end{cases} \quad (3)$$

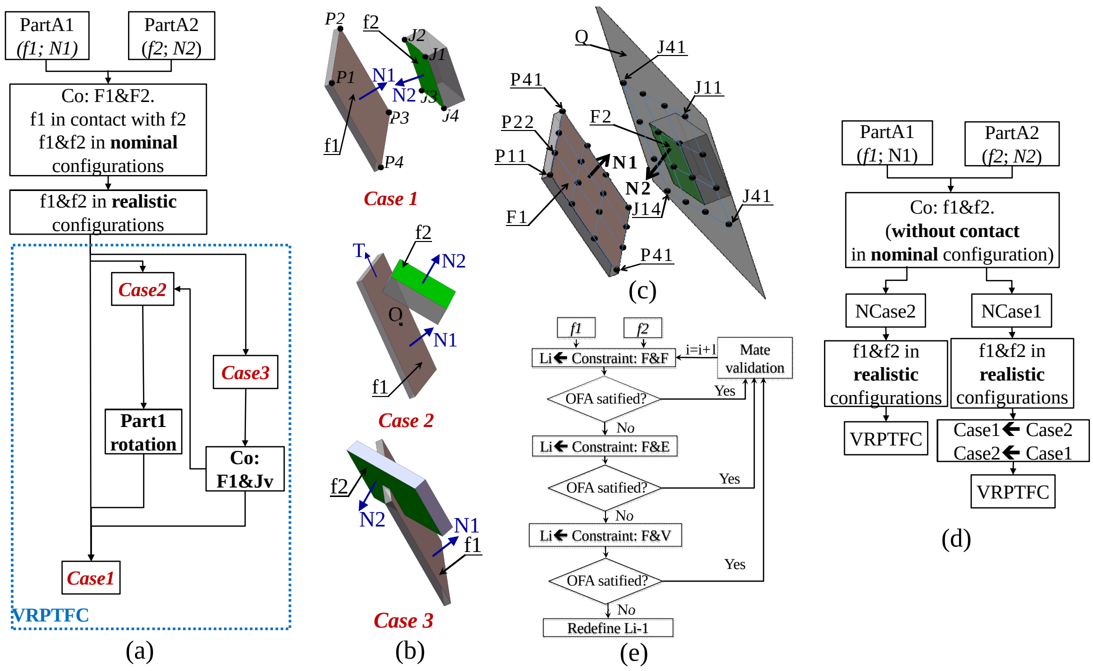

FIG. 2 – (a) The sub- algorithm VRPTFC, (b) Three initial cases identified by the sub- algorithm VRPTFC, (c) Determination of the tangent vertex between two faces by the surface modelling by a gird, (d) The sub-algorithm VRPTFWC, (e) Sub-algorithm to identify constraint type between two planar faces initially on distance or coincident relationship.

Then, the mating constraints are conserved (Co: *F&F*) or replaced by the assembly constraints which allow more DoF ((Co: *F&V*) or (Co: *F&E*)) according to the OFA (Fig. 2(e)):

*Case of Co:F&V***:** To apply a coincident constraint between *f1* and a vertex *Sa* of *f2*, a vertex *Sa* is to be identified. Initially, *f2* is discretized. The discretization method depends on the type of the face loop. In the case of quadratic loop the discretization is performed by two parameters *n* and *m* (Fig. 2 (c)). The face with circular contour is discretized by two polar parameters *r* and *θ*. For the face with complex loop, the discretization is performed by a fine tessellation. These discretization parameters are chosen by the designer according to the desired accuracy of the results. The explication will be limited to the case of face with quadratic loop. *f1* is modelled by a grid of P_{nm} vertices. Then, all P_{nm} vertices are projected on the plane *Q* according to *N1* to obtain the set of J_{nm} vertices. Finally, the distance d_{min} is the minimum distance between the pairs (P_{nm}, J_{nm}) and the vertex *Sa* is identified by the relation (Eq. 4).

$$\begin{cases} d_{\min} = \min \left\| \overrightarrow{J_{nm}P_{nm}} \right\|; \text{ such as } J_{nm} \in \text{f2} \\ \text{Sa}=J_{nm}; \text{ such as } \left\| \overrightarrow{J_{nm}P_{nm}} \right\| = d_{\min} \end{cases} \quad (4)$$

Case of Co:F&E: To determine the edge *E* it suffices to identify the two vertices *V1* and *V2* (*E*= [*V1V2*]). The face *f2* is discretized by using the method described previously. The first vertex *V1* is determined by the relation (Eq. 4). The second vertex *V2* is identified by the equation (Eq. 5).

$$\begin{cases} d'_{\min} = \min \left\| \overrightarrow{J_{nm}P_{nm}} \right\|; \text{ such as } J_{nm} \in \text{f2 and } J_{nm} \neq \text{Sa} \\ \text{V2}=J_{nm}; \text{ such as } \left\| \overrightarrow{J_{nm}P_{nm}} \right\| = d'_{\min} \end{cases} \quad (5)$$

b. The case of two planar face without contact in the nominal configuration

In the nominal assembly, a coincident constraint between two faces *f1* and *f2* of two parts *A1* and *A2* is applied such as the two faces are not in contact. *N1* and *N2* are the two normal vectors of *f1* and *f2* respectively. Both faces can have two main initial configurations NCase1 and NCase2 defined by the relation (Eq. 6). The relative position of the two faces in the nominal configuration must be respected in the realistic one. In the realistic assembly, the relative position of *f1* and *f2* is verified by using a sub-algorithm to Verify Relative Position of Two Faces initially Without Contact (VRPTFWC) (Fig. 2(d)). In the realistic configuration, the two faces can be in one of the three cases described in Fig. 2 (b). In the case NCase2, the method is similar to the method defined previously: the sub-algorithm VRTFC is used. In the case NCase1, the case2 becomes the optimal case (Fig. 2(d)). Then, the sub-algorithm VRTFC is used after replaced the condition and the statement of the case1 by the condition and the statement of the case2. In realistic modelling, the mating constraint Co: *F&V,* Co: *F&E* or Co; *F&F* are to be applied in realistic model according to OFA (Fig. 2(e)):

$$\begin{cases} \text{If } \overrightarrow{N1}.\overrightarrow{N2}=1, \text{ then NCase1} \\ \text{If } \overrightarrow{N1}.\overrightarrow{N2}=-1, \text{ then NCase2} \end{cases} \quad (6)$$

In the case of Co:*F&V*, the method used is similar to the previously one (Case of faces initially in contact); such as *Sa* can be outside the face *f2*. Also, in the case of Co:*F&E:* The method is similar to the previously one (Case of faces initially in contact). The first vertex *V1* is determined by the relation (Eq. 4). The second vertex *V2* is identified by the equation (Eq. 5); such as J_{nm} can be outside the face *f2*.

3.1.2 A distance constraint between planar faces

In the nominal assembly, a distance mate between two faces *f1* and *f2* of two parts *A1* and *A2* is applied. In the realistic assembly, the relative position of *f1* and *f2* is verified by using a sub-algorithm VRPTFC. In the realistic configuration, the distance constraint, which is defined in nominal configuration between two planar faces (Dist: *F&F*), will be conserved or replaced by a distance mate between a planar face and an edge (Dist: *F&E*) or by a distance mate between a planar face and a vertex (Dist: *F&V*) according to the OFA (Fig. 2(e)). The definition of the mates (Dist: *F&E*) and (Dist: *F&V*) is performed as the method used to define the mating constraints (Co: *F*&E) and (Co: *F&V*) in the case of the coincidence mates between planar faces initially in contact (section 3.1.1 a).

3.1.3 Application

For the mechanical system of the figure 1 (b), the parts *1* and *2* are linked by the three constraints *L1*, *L2* and *L3*. In the realistic model, the parts *1* and 2 become the realistic parts *1'* and *2'* respectively: *F11*, *F12*, *F13* and *C21* become *F'11*, *F'12 F1'3* and *C'21* respectively (Fig. 3 (a)). To update those three constraints, the others assembly relations are deactivated temporarily (*Li*; *i*=4 to 9). According the method detailed previously, the fixed joint between the realistic parts *1'* and *2'* is realized by the three constraints: *L1* (Co: *F21&F'11*), *L'2* (Co: *F22&E1*) and *L'3* (Co: *F23&V1*). In addition, the fixed joint between the parts *1'* and *3'* (*C'41* is the realistic face obtained from *C41*) is performed by the three constraints: *L4* (Co: *F41&F'11*), *L'5* (Co: *F42&E2*), *L'6* (Dist: *F43&V2*) (Fig. 3 (b)).

3.2 The case of cylindrical, revolute or fixed joints performed by coincident constraints between axes and between planar faces in contact

In the realistic model, a coincident constraint between two axes (a coaxiality relation), defined in nominal configuration, is specified by the coincident constraint between: axis and axis (Co: *A&A*) or axis and vertex (Co: *A&V*). The method is shown through the case of revolute and cylindrical joint between the part couples (*2, 3*) and (*3, 4*) respectively (Fig. 1 (b)). These two joints define an attachment relation. The realistic component *4'* is deduced from the part *4* by the displacements of the cylindrical faces *C31* and *C32*. Thus, the faces *C'31* and *C'32* are deduced from *C31* and *C32* respectively. Let *A'31* and *A'32* the axes of *C'31* and *C'32* respectively. In the realistic configuration of the assembly, if *L'7* is defined as (Co: *A'31&A21*), then the addition of a constraint (Co: *A&A* or Co: *A&V*) to link the parts *3'* and *4'* over constraint the assembly. Therefore, *L'7* is redefined as (Co: *A'31&V3*). *V3* is a vertex on the *A'21* axis (*A'21* is a realistic configuration of *A21* and *A'21* is descretized to obtain a vertex set. *V3 ϵ A'21*). Then, *L8* is replaced by the constraint *L'8* (Co: *A'32&V4*). The *V4* vertex can be one the vertices obtained by the discretization of *A'42* (*A'42* is a realistic configuration of *A42*). The constraint *L9* (*Co: F31&F22*) is substituted by *L'9* coincident constraint between the *Q1* plane and the *Vnm* vertex. To determine *Vmn* and *Q1*, a method was developed (Fig. 3(c)): The face *F5* is modelled by a gird of *Pij* vertices (method detailed previously). *Pij* are projected on the axis *A* (*A*=*V3V4*: the rotation axis of the part *4'*) to obtain the *Kij* vertices (Fig. 3(d)). The vertex *O* is the intersection between the axis *A* and the face *F22*. The plane *Q1* is perpendicular to *A* through *Vmn*. The vertex *Vmn* is the projection of *Pmn* on *F31* along the face normal vector N. Then, a coincident constraint is applied between the plane *Q1* and the vertex *Vmn* (Fig. 3 (e)). In realistic model, the interferences are detected when the axis rotation is simulated. Then, the redefinition of the geometrical and dimensional tolerances is necessary. The proposed method is a tolerance analysis tool.

In the case of a revolute joint between two parts defined by two constraints L1 (Co: *A&A*) and L2 (Co: *P&P*), the realistic assembly of these two parts is defined by L1 and L'2 (Co: *P&V*). The *V* vertex is determined by using the method shown in Fig. 3 (c).

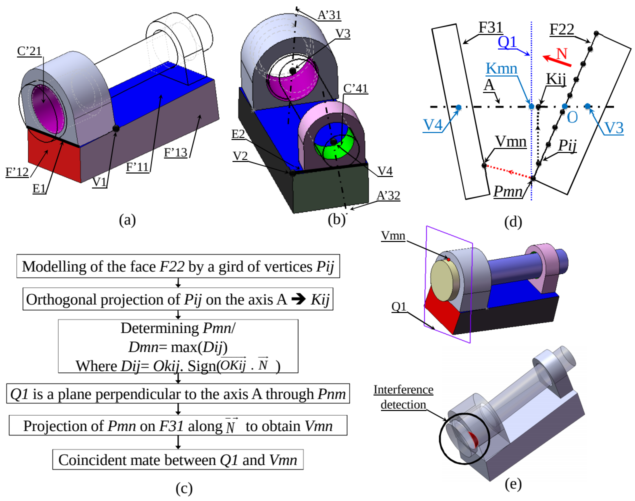

FIG. 3 – (a) Realistic assembly with L'1, L'2 and L'3, (b) Realistic assembly with L'i (i=1 to 6), (c) Identification method of Q1 and Vmn, (d) 2D modelling of the method. (e) Realistic assembly with all mating constraints

4 Conclusion

In this paper, a method to incorporate the dimensional and geometrical tolerances in CAD model is presented. These realistic assemblies are obtained by determining the possible configurations of the components which are allowed by the tolerances. In the DMU, the model rebuilt requires the updating of the mating constraints that are initially defined in the nominal model. The redefinition of these assembly constraints are realized according to the OFA of the mechanism. The method for constraints updating is shown through a mechanical assembly. The proposed model is under improvement through the applications on complex assemblies. The model is an improvement of the DMU by allowing the tolerance analysis. In addition, the tolerance impacts on the results of F.E. calculation or dynamic computation can be performed. However, the form specifications can have effects on assembly requirements. Then, the current research works are interested in the consideration of the form defects on CAD model through another type of the tolerancing approach [13].

References

[1] Clozel P, Rance P-A, MECAmaster: A Tool for Assembly Simulation from Early Design, industrial approach, Chapter 10 in: Geometric tolerancing of products, Villeneuve F., Mathieu L. (eds), May 2010.
[2] Anselmetti B., Louati H., Generation of manufacturing tolerancing with ISO standards, International Journal of Machine Tools & Manufacture, vol. 45, pp. 1124–1131, 2005.
[3] Germain F., Giordano M., A new approach for three-dimensional statistical tolerancing, CIRP'07, Germany, 2007.
[4] Pillet M., Adragna P.A., Germain F., Inertial Tolerancing: The Sorting Problem, Journal of Machine Engineering: Manufacturing Accuracy Increasing Problems, Optimization, Vol.6, No. 1, pp. 95-102, 2006.
[5] Socoliuc M., Buysse D., Riviere A., Towards a new digital functional validation process, CPI'07, Morocco, 2007.
[6] Clement A., Riviere A., Serre P., The TTRS : a common declarative modal for relative positioning, tolerancing and assembly', International journal of CAD/CAM and computer graphics, vol. 11, pp. 149-164, 1996.
[7] Petit J-Ph., Samper S., Tolerancing analysis and functional requirement, IDMME'04, 2004, paper 205.
[8] Pierre L., Teissandier D., Nadeau J.P., Integration of thermomechanical strains into tolerancing analysis, International Journal on Interactive Design and Manufacturing, Vol. 3, pp. 247-263, 2009.
[9] Saka A., Boutahari S., Radouani M., Carrard M., Numerical study in VD&T manufacturing analysis for tolerance synthesis', Revue Internationale d'Ingénierie Numérique, Vol 2, n° 1-2, pp. 89-111, 2006.
[10] Louhichi B, Tlija M., BenAmara A., Francois V., Reconstruction d'un modèle CAO à partir d'un maillage déformé - Application dans le cas de grands déplacements, Mécanique & Industries, vol. 10, p 477–486, 2009.
[11] Tlija M., Louhichi B., Benamara A., Integration of tolerances in the mechanical product process, IMProVE'11, 2001, pp. 499-506.
[12] Tlija M., Louhichi B., Benamara A., Une méthodologie de modélisation et simulation des assemblages réalistes, CPI'09, 2009, paper 34.
[13] S. Samper, P-A. Adragna, H. Favreliere, M. Pillet, Modeling of 2D and 3D Assemblies Taking Into Account Form Errors of Plane Surfaces, Journal of Computing and Information Science in Engineering 9, 4 (2009) 041005.